Mitotic chromatin regulates phosphorylation of Stathmin/Op18

Søren S. L. Andersen*, Anthony J. Ashford, Régis Tournebize, Olivier Gavet†, André Sobel†, Anthony A. Hyman‡ & Eric Karsenti‡

EMBL, Cell Biology Programme, Meyerhofst. 1, D-69117 Heidelberg, Germany
† INSERM U440, 17, rue du Fer à Moulin, F-75005 Paris, France

Meiotic and mitotic spindles are required for the even segregation of duplicated chromosomes to the two daughter cells. The mechanism of spindle assembly is not fully understood, but two have been proposed that are not mutually exclusive[1–3]. The 'search and capture' model suggests that dynamic microtubules become progressively captured and stabilized by the kinetochores on chromosomes, leading to spindle assembly[3,4]. The 'local stabilization' model proposes that chromosomes change the state of the cytoplasm around them, making it more favourable to microtubule polymerization[2,5–9]. It has been shown[10,11] that Stathmin/Op18 inhibits microtubule polymerization *in vitro* by interaction with tubulin[12], and that overexpression in tissue culture cells of non-phosphorylatable mutants of Stathmin/Op18 prevents the assembly of mitotic spindles[13]. We have used *Xenopus* egg extracts and magnetic chromatin beads[14] to show that mitotic chromatin induces phosphorylation of Stathmin/Op18. We have also shown that Stathmin/Op18 is one of the factors regulated by mitotic chromatin that governs preferential microtubule growth around chromosomes during spindle assembly.

It has recently been shown that Stathmin/Op18 is involved in the regulation of microtubule dynamics and spindle assembly[12,13]. We therefore decided to examine the regulation of its phosphorylation during the transition from interphase to metaphase in *Xenopus* egg extracts. The analysis of immunoprecipitates of Stathmin/Op18 from interphase and mitotic egg extracts by SDS–PAGE (polyacrylamide gel electrophoresis) revealed a triplet (Fig. 1a). Two-dimensional gel electrophoresis of the same immunoprecipitates revealed four spots (Figs 1b, 2b). We could not detect any difference between interphase and mitotic immunoprecipitates using either of these techniques. Treatment of the immunoprecipitates with alkaline phosphatase reduced the triplet to one band using SDS–PAGE (data not shown), and the four spots to two using two-dimensional gel electrophoresis, indicating that both interphase and mitotic extracts contain two partly phosphorylated Stathmin/Op18 isoforms, referred to as n1, n2, p1, p2 (refs 10, 15) (Fig. 1b). However, there was no significant incorporation of phosphate into interphasic or mitotic Stathmin/Op18, indicating a low phosphate turnover rate (Fig. 1a). Taken together, these results indicate that Stathmin/Op18 is not differentially phosphorylated between interphase and mitosis in *Xenopus* egg extracts.

This was surprising given a previous report showing that Stathmin/Op18 is hyperphosphorylated in mitotic cells[13]. We wondered whether the lack of difference in Stathmin/Op18 phosphorylation between interphase and mitotic extracts was due to the absence of nuclei in these extracts. To test this idea we added increasing amounts of chromatin beads from interphase or mitosis to interphase and mitotic extracts. The addition of interphase bead nuclei to an interphase or to a mitotic extract did not result in an increase in Stathmin/Op18 phosphorylation (Fig. 1c and data not shown). However, two additional bands that incorporated ^{32}P appeared on SDS–PAGE of immunoprecipitates following the addition of mitotic chromatin beads to a mitotic extract (Fig. 1c). Hyperphosphorylation of Stathmin/Op18 was dose dependent and reached a maximum at 50,000–100,000 mitotic chromatin beads per 1-μl extract, which corresponds to 5,000–10,000 nuclei per 1-μl extract (Fig. 1d, e).

We did not detect any significant incorporation of phosphate into Stathmin/Op18 in mitotic extracts lacking chromosomes (n1, n2, p1, p2; Fig. 1), so we suspected that the chromatin beads induced the hyperphosphorylation of Stathmin/Op18 by changing the balance between the activity of phosphatases and kinases in the extract. To investigate the role of phosphatases in determining the phosphorylation state of Stathmin/Op18, we added phosphatase

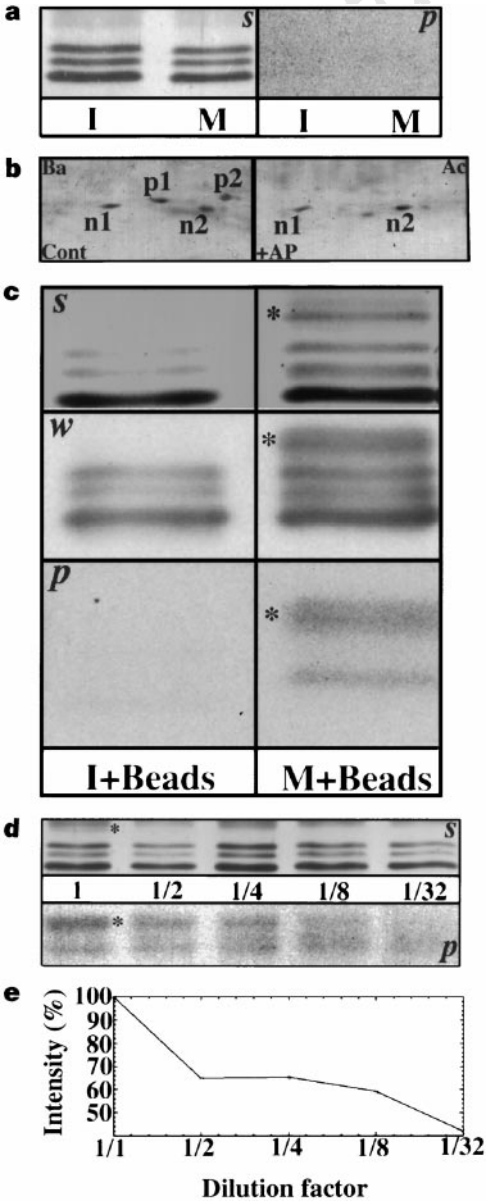

Figure 1 Hyperphosphorylation of Stathmin/Op18 during mitosis requires mitotic chromatin. **a**, [γ-^{32}P]ATP-labelled Stathmin/Op18 from interphase (I) and mitotic (M) extracts; s, silver staining; p, autoradiography, 15% SDS–PAGE. **b**, Two-dimensional gels of purified mitotic Stathmin/Op18 treated without (Cont) or with alkaline phosphatase (+AP) reveals n1, n2, p1, p2; n, non-phosphorylated; p, phosphorylated; Ba, basic; Ac, acidic. **c**, Stathmin/Op18 hyperphosphorylation and two high-molecular-weight forms (asterisks) during mitosis (M + Beads), but not interphase (I + Beads); w, western blot. **d**, Mitotic chromatin beads resuspended at 50,000–100,000 beads per 1 μl extract (1), diluted (dilution factor) with extract, and then [γ-^{32}P]ATP-labelling for 15 min. **e**, Quantification of d.

* Present address: Department of Molecular Biology, Princeton University, Princeton, New Jersey 08544-1014, USA.
‡ These authors contributed equally to this work.

inhibitors to interphase and mitotic extracts. Inhibition of type 2A phosphatases (PP2A)[16] with 0.5 μM okadaic acid in interphase extracts had no effect on the phosphorylation of Stathmin/Op18 (data not shown). However, in mitotic extracts, this resulted in an SDS–PAGE phosphorylation pattern identical to that produced by adding mitotic chromatin (Fig. 2a). Total inhibition of phosphatase 1 with 3 μM inhibitor 2 had no significant effect on Stathmin/Op18 phosphorylation[17]. By two-dimensional gel electrophoresis, Stathmin/Op18 resolved as six spots after treatment with okadaic acid or mitotic chromatin (Fig. 2b). The clearest difference between control extracts and extracts treated with mitotic chromatin or okadaic acid was the appearance of two extra phosphorylated Stathmin/Op18 spots, termed p3 and p4, which probably arise from the phosphorylation of p1 and p2 (Fig. 2b). This result could mean that Stathmin/Op18 is actively dephosphorylated by PP2A, or that Stathmin/Op18 becomes phosphorylated because inhibition of PP2A activates a kinase that phosphorylates Stathmin/Op18, or the mechanism may be more complex. To test these possibilities, we added *in vivo* phosphorylated Stathmin/Op18 to mitotic extracts, and observed that 0.5 μM okadaic acid blocked dephosphorylation (Fig. 2c). When this experiment was repeated with chromatin beads instead of okadaic acid, we did not detect a significant block of Stathmin/Op18 dephosphorylation (data not shown). However, we measured[18] an approximately 10% reduction in total PP2A activity in the presence of high concentrations of mitotic chromatin beads, but did not detect any change in the Cdc2 kinase activity (data not shown). Thus the mechanism by which chromatin induces Stathmin/Op18 phosphorylation remains unclear.

In order to investigate which of the three *Xenopus* Stathmin/Op18 (ref. 15) phosphorylation sites were actively phosphorylated in the extract, we mutated all three serines to alanines in all possible combinations, and added endogenous amounts of the recombinant proteins to interphase and mitotic extracts in the presence of [γ-^{32}P]ATP (Fig. 3). No incorporation of phosphate was observed when all three serines were mutated (Δall), showing that Ser 16 (PKA site), Ser 25 (MAPK site) and Ser 39 (Cdc2 site)[15] can account for the phosphorylation patterns observed in both interphase and mitotic extracts. Addition of mutants with only one functional site to interphase and mitotic extracts revealed that only Ser 39 incorporates phosphate (Fig. 3). However, in interphase, both a functional Ser 16 and a functional Ser 39 are required for a wild-type phosphorylation level of Stathmin/Op18, whereas Ser 25 appears dispensable (Fig. 3). In mitosis, either Ser 16 or Ser 25, together with Ser 39, is required to obtain wild-type phosphorylation levels (Fig. 3, quantification not shown). These results indicate that the Cdc2 site (Ser 39) is the principal site phosphorylated in mitosis, and that there is some degree of cooperativity between the phosphorylation of Ser 39 and Ser 16/Ser 25, as previously proposed[19].

The previous results indicated that the activity of Stathmin/Op18 could be regulated by phosphorylation. To address this question we tested the effect on spindle stability of mutant Stathmin/Op18 containing all phosphorylation sites changed to alanines. The addition of this mutant to preassembled spindles resulted in a reduction of microtubule mass, decreasing spindle size significantly (by 20%) compared with those after the addition of an equivalent amount of wild-type Stathmin/Op18 (Fig. 4A, B; graphs are based on measurement of 2,320 spindles, and the s.d. of each point was 5–7 μm). At mutant protein concentrations above 200 μg ml^{-1}, spindle stability was strongly affected, causing a collapse of most of the spindles (the endogenous Stathmin/Op18 concentration is 5–6 μM, or 100 μg ml^{-1}; data not shown and ref. 12). We determined that the observed spindle shortening occurs within 3 min of Stathmin/Op18 addition (Fig. 4B), which is in the range of microtubule half-life in spindles assembled *in vitro*[20]. Addition of Stathmin/Op18 during spindle assembly had the same effect (data not shown). These data indicate that phosphorylation of Stathmin/Op18 is required to turn off its inhibitory effect on microtubule polymerization[13]. Because adding Stathmin/Op18 results in spindle shortening we thought that removing Stathmin/Op18 might result

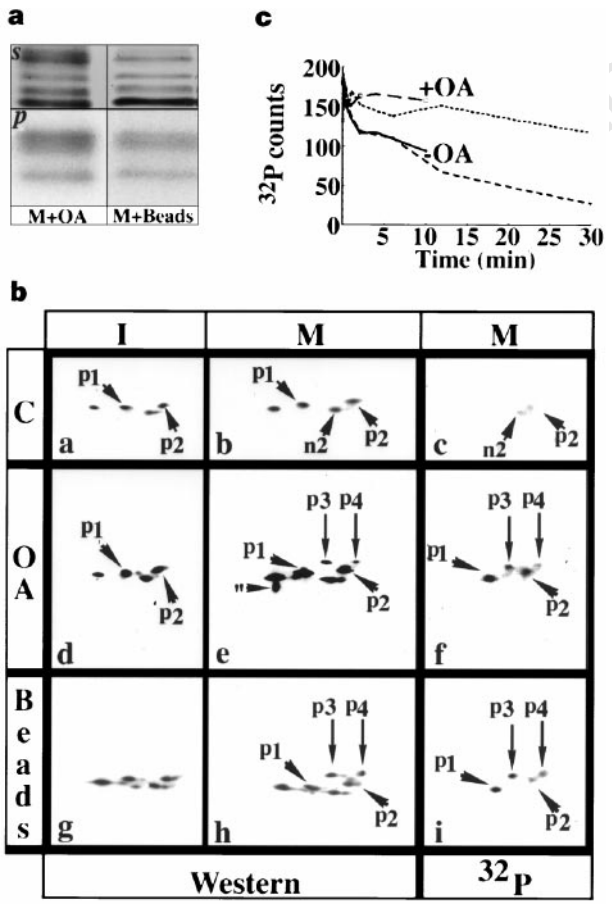

Figure 2 A type 2A phosphatase regulates Stathmin/Op18 phosphorylation. **a**, Stathmin/Op18 from mitotic extracts treated with chromatin (M + Beads) or 0.5 μM okadaic acid (M + OA); s, silver staining; p, autoradiography, 15% SDS–PAGE. **b**, Two-dimensional (right, acidic end) phosphorylation pattern of Stathmin/Op18; control (c), okadaic acid (OA) and chromatin bead (Beads) treatment in interphase (I) or mitotic (M) extracts; p3 and p4 only appear after treatment with OA or mitotic chromatin beads, also required for ^{32}P-labelling of p1 and p2. Note the more complex pattern with OA than mitotic chromatin, notably a non-reproducible spot (II); Western, western blotting; ^{32}P, autoradiography. **c**, Dephosphorylation of Stathmin/Op18 is blocked by 0.5 μM okadaic acid in mitotic extracts.

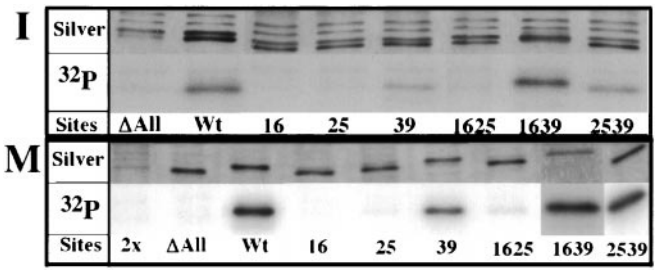

Figure 3 Stathmin/Op18 is phosphorylated mainly on the Cdc2 site in mitosis. Constructs of Stathmin/Op18 were added to an interphase (I) and a Stathmin/Op18-depleted mitotic extract (M) for 15 min together with 1 μCi [γ-^{32}P]ATP per 1-μl extract, and then immunoprecipitated (15% SDS–PAGE; Silver, silver staining; ^{32}P, autoradiography). See text for sites. 2× indicates double depletion without addition of recombinant protein. Addition of proteins to a non-depleted mitotic extract gave similar results. In interphase, phosphorylation on the Cdc2 site could be due to a kinase other than Cdc2. In the presence of 0.5 μM okadaic acid, no specific site showed a significant increase in ^{32}P incorporation, but p3 and p4 forms were observed.

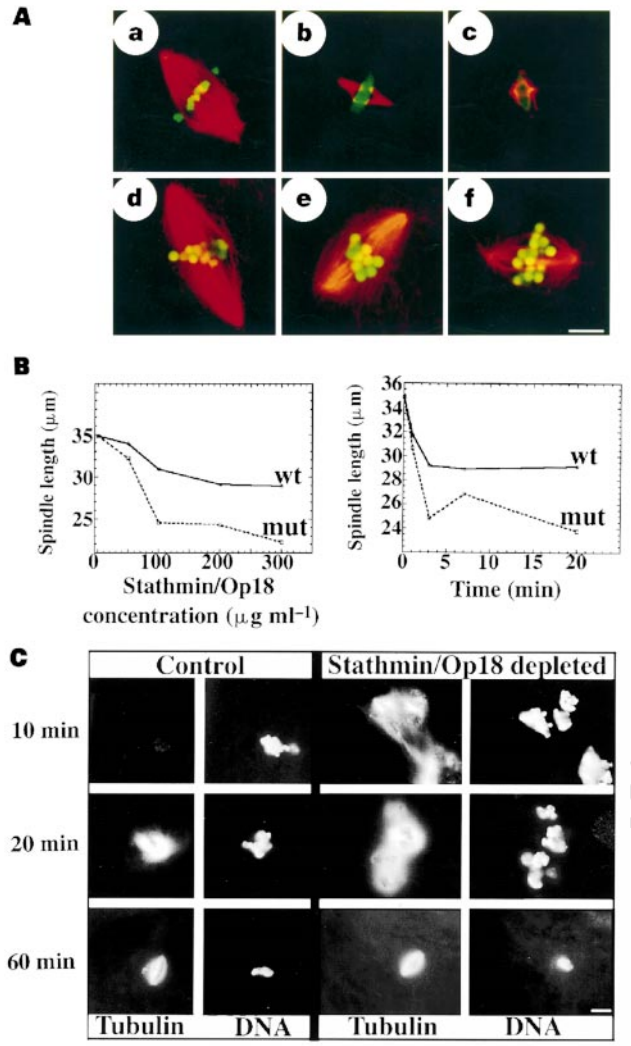

Figure 4 Mutant Stathmin/Op18 causes rapid shortening of the mitotic spindle. **A**, **B**, Pre-formed mitotic sperm and bead spindles were incubated with 100 (**a**, **d**), 200 (**b**, **e**) and 300 (**c**, **f**) μg ml^{-1} mutant Stathmin/Op18, fixed after 20 min, and the mean spindle length was measured (DNA, green; microtubules, red); scale bar, 5 μm. **B**, Quantification of the sperm spindles shown in A; using wild-type (wt) and mutant (mut) Stathmin/Op18. Left, length; right, time, for which 100 μg ml^{-1} Stathmin/Op18 was used. **C**, Immunoprecipitation of Stathmin/Op18 results in accelerated microtubule nucleation around mitotic chromatin. Mitotic chromatin was added to control or Stathmin/Op18-depleted extracts and time points taken. Addition of recombinant wild-type *Xenopus* Stathmin/Op18 to *in vivo* concentrations rescued the effect of immunodepletion. Scale bar, 25 μm.

in promotion of microtubule assembly and nucleation. Immunodepletion[12] of 90–95% of Stathmin/Op18 from the extract had a significant effect during the early stages of spindle assembly, when large sperm microtubule asters were observed (Fig. 4C), as previously described[12]. Moreover, we observed an acceleration in microtubule formation around mitotic chromatin beads (approximately 10–20 min; Fig. 4C). However, at later stages of bead and sperm spindle assembly there were no differences between the Stathmin/Op18 depleted and non-depleted extracts (Fig. 4C), and direct measurements of microtubule dynamics have shown that Stathmin/Op18 is not the principal regulator of microtubule catastrophes in extracts[17] or *in vitro*[30]. These data suggest that, although lowering the concentration of Stathmin/Op18 affects microtubule dynamics in the extract, as well as the kinetics of the early stages of spindle assembly[8], microtubule dynamics are regulated by other factors, still allowing spindle assembly. One candidate molecule is XKCM1, a *Xenopus* kinesin-like protein that increases the frequency of catastrophes and is required for spindle assembly[21]. XKCM1 and other factors may make microtubules sufficiently dynamic to allow assembly of mitotic spindles in the absence of Stathmin/Op18.

The most striking observation is that mitotic chromatin causes a dose-dependent increase in the phosphorylation level of Stathmin/Op18. Although we do not understand exactly how this is achieved, our data strongly suggest that a type 2A phosphatase (PP2A)[16] and Cdc2 kinase are involved. Indeed, when PP2A is inhibited in mitotic extracts, phosphorylation of Stathmin/Op18 probably occurs through Cdc2 kinase, as the Cdc2 site is the main site phosphorylated, and inhibition of PP2A in interphase extracts does not result in hyperphosphorylation (data not shown). We can think of two possible mechanisms to explain how mitotic chromatin could induce the phosphorylation of Stathmin/Op18 in mitotic extracts. The simplest mechanism would involve an activity present on chromosomes that blocks PP2A, which dephosphorylates Stathmin/Op18. But this seems to be in contradiction with the lack of inhibition of Stathmin/Op18 dephosphorylation by chromatin beads. The other possibility is that a kinase[22] present on chromosomes (perhaps activated by partial PP2A inhibition) is responsible for the phosphorylation of Stathmin/Op18. This mechanism could explain why mitotic chromatin does not significantly block Stathmin/Op18 dephosphorylation in the extract. Further work will be needed to determine the details of this pathway. The progressive increase in Stathmin/Op18 phosphorylation, which parallels the number of beads added to the extracts, suggests that there is a gradient of Stathmin/Op18 phosphorylation/activity around chromosomes. This may be part of a general mechanism involved in regulating preferential microtubule growth around chromosomes during spindle assembly. Chromatin may also regulate the phosphorylation of Stathmin/Op18 during mitosis in other systems[13]. Moreover, in the absence of chromosomes, endogenous Stathmin/

Op18 is phosphorylated to the same extent in both interphase and mitosis (Fig. 1a), suggesting that its main function is not to regulate the global change in microtubule dynamics that occurs during the transition from interphase to mitosis[11–13]. Rather, we think this change is caused by global phosphorylation of microtubule-associated proteins, which reduces their affinity for microtubules[23–25], allowing destabilizing factors to make microtubules more dynamic.

We predict that other molecules involved in the regulation of microtubule assembly are regulated in a similar manner to Stathmin/Op18. Good candidate molecules include spindle-associated microtubule-associated proteins[23–25], as well as the spindle-associated motor proteins XKCM1, XKLP1 and CENP-E[21,26,27]. □

Methods

Extracts and spindles. *Xenopus* egg extracts (10,000*g*) arrested in the second meiotic metaphase (CSF extracts; H1 kinase activity, 15–30 pmol μl min^{-1}; ref. 28) for sperm, magnetic bead spindle and magnetic interphase bead nuclei (50% competent for nuclear transport) assembly were prepared fresh and cycled as described[14,29]. For interphase extracts (H1 kinase activity, 2–4 pmol μl^{-1} min^{-1}), eggs were activated for 15 min in MMR/4, 0.2 μg ml^{-1} A23187 (Sigma), 200 μg ml^{-1} cycloheximide. When spindles had assembled (Fig. 4A), 1/10 volume control buffer, wild-type or mutant Stathmin/Op18 diluted in CSF-XB was added. Purified wild-type and mutant (serines changed to alanines at positions 16, 25, 38 and 63) human Stathmin/Op18 (from A. Sobel) were in PBS at 10 mg ml^{-1}.

Immunoprecipitations. Extracts 5–40 μl were labelled with 1 μCi [γ-^{32}P]ATP per μl extract for 15 min at 20 °C. For the immunoprecipitation, 2–10 volumes cold SBMI (100 mM NaF, 80 mM β-glycerophosphate, 20 mM $Na_2P_2O_7$, 20 mM EDTA, pH 7.2, with 1 μM microcystin-LR (Gibco BRL), 1 mM PMSF and 10 μg ml^{-1} each of leupeptin, pepstatin and aprotinin) containing Affi-prep protein A beads (Biorad) with rabbit anti-Stathmin/Op18 antibodies precoupled (partial gift from T. J. Mitchison[12]) was added for 30 min at 4 °C, followed by two washes with 200 μl SBMI, four washes with 200 μl PBS plus 100 mM NaCl, 0.1% Tx-100, protease inhibitor mix. When present, magnetic beads were removed after SBMI addition but before the immunoprecipitation. In the presence of okadaic acid, Δ90CyclinB was added to the CSF extracts to prevent inactivation of Cdc2 kinase. Interphase bead nuclei added for <5 min, fresh DNA beads, or polyglutamic acid control beads added to a mitotic or interphase extract had no effect on phosphorylation (Fig. 1, data not shown).

Statistics. Comparison of spindle length in the presence of wild-type and mutant Stathmin/Op18; A χ^2-test verified that spindle lengths follow a normal distribution, and Bartlett's test showed that the standard deviations are equal. The statistical test subsequently consisted of a *t*-test, $t = (\mu_1 - \mu_2)/[s(1/n_1 + 1/n_2)^{1/2}]$. $P > 95\%$ ($P < 0.05$) is considered statistically significant.

***Xenopus* Stathmin/Op18 cloning and expressions.** The 5′ and 3′ oligonucleotides used for PCR cloning of *Xenopus* Stathmin/Op18 (XLXO35)[15] contained a *Nde*I and a *Hin*dIII site, respectively: GGGAATTCC ATATGTGTGACTCTGATATTAAAGTAAAACAGC and CCAAGCTTCTATC ACTTCTCAGAAGGTTCTTTGCATTC. A *Xenopus* cDNA library was prepared using purified polyadenylated RNA (RNeasy, Qiagen) from XL177 cells and a cDNA synthesis kit (Boehringer-Mannheim). *Xenopus* Stathmin/Op18 was subcloned into pMW172. Mutagenesis of *Xenopus* Stathmin/Op18 was performed according to the Quickchange site-direct mutagenesis kit protocol (Stratagene). All constructs were sequenced in pMW172 from the T7 promoter (EMBL sequencing service). *Xenopus* Stathmin/Op18 was expressed in *Escherichia coli* (BL21DE3), induced at 0.3–0.5 absorbance at 600 nm (0.1 mg ml^{-1} IPTG) for 3 h at 37 °C.

Purifications. Pellets from 1–2 l of cells were sonicated on ice for 3 × 20 s in 50–100 ml 20 mM Tris-HCl pH 8.3, 1 mM EGTA, 1 mM EDTA, 0.1% β-mercaptoethanol, and protease inhibitor mix. This was centrifuged at 30,000*g* for 10 min at 4 °C, and batch-absorbed to 10–20ml DEAE (Pharmacia) in 20 mM Tris, pH 7, 200 mM NaCl for 20 min at 4 °C. DEAE was removed (4,000*g*, 10 min, 4 °C), the supernatant filtered through Kleenex paper, and ammonium sulphate powder was added to 60% for 30 min at 4 °C. The $(NH_4)_2SO_4$ pellet was recovered by centrifugation at 15,000*g*, 10 min, 4 °C, then resuspended in 5–10 ml 30 mM K-MES, pH 5.7, 0.1% β-mercaptoethanol and protease inhibitor mix, and dialysed overnight at 4 °C against 400 volumes of the same buffer. The dialysate was centrifuged at 14,000*g*, 10 min, 4 °C, loaded onto a Mono-S PC 1.6/5 SMART column (Pharmacia) equilibrated with buffer A (20 mM K-MES, pH 5.7). Stathmin/Op18 was eluted with a step-gradient in 100 μl at 25% buffer B (buffer A with 500 mM NaCl). The yield never exceeded 200 μg per litre of cells (BCA; Pierce).

Dephosphorylation. Stathmin/Op18 was 100-fold purified from 2 × 600 μl okadaic acid-treated [γ-^{32}P]ATP-labelled mitotic extract; 5 volumes SBMI was added after 15 min labelling, and the mix was heated at 95 °C for 5 min, centrifuged at 100,000*g*, 10 min, 2 °C, followed by 5-fold concentration in Centricon-30, desalting into CSF-XB on a 5-ml Kwiksep column (Pierce), and 2-fold concentration in Centricon-30. This concentrate was mixed at a maximum dilution ratio of 1 : 1 with extracts and samples taken into sample buffer (Fig. 2c).

Miscellaneous. Pure Stathmin/Op18 (Fig. 1b) was obtained by immunoprecipitation, elution for 1 h at 4 °C with 200 μg ml^{-1} anti-Stathmin/Op18 peptide[12] in XB, dilution with 10 volumes XB, concentration on Centricon-10 and incubation with 2 units alkaline phosphatase μl^{-1} for 1 h at 37 °C.

Received 7 May; accepted 7 July 1997.

1. Waters, J. C. & Salmon, E. D. Pathways of spindle assembly. *Curr. Opin. Cell Biol.* **9,** 37–43 (1997).
2. Hyman, A. A. & Karsenti, E. Morphogenetic properties of microtubules and mitotic spindle assembly. *Cell* **84,** 401–411 (1996).
3. Nicklas, R. B. How cells get the right chromosomes. *Science* **275,** 632–637 (1997).
4. Kirschner, M. W. & Mitchison, T. J. Beyond self assembly: from microtubules to morphogenesis. *Cell* **45,** 329–342 (1986).
5. Marek, L. F. Control of spindle form and function in Grasshopper spermatocytes. *Chromosoma* **68,** 367–398 (1978).
6. Karsenti, E., Newport, J. & Kirschner, M. Respective roles of centrosomes and chromatin in the conversion of microtubule arrays from interphase to metaphase. *J. Cell Biol.* **99,** 47s–57s (1984).
7. Nicklas, R. B. & Gordon, G. W. The total length of spindle microtubules depends on the number of chromosomes present. *J. Cell Biol.* **100,** 1–7 (1985).
8. Zhang, D. & Nicklas, R. B. The impact of chromosomes and centrosomes on spindle assembly as observed in living cells. *J. Cell Biol.* **129,** 1287–1300 (1995).
9. Zhang, D. & Nicklas, R. B. Chromosomes initiate spindle assembly upon experimental dissolution of the nuclear envelope in grasshopper spermatocytes. *J. Cell Biol.* **131,** 1125–1131 (1995).
10. Sobel, A. Stathmin: a relay phosphoprotein for multiple signal transduction? *Trends Biochem. Sci.* **16,** 301–305 (1991).
11. Belmont, L., Mitchison, T. & Deacon, H. W. Catastrophic revelations about Op18/stathmin. *Trends Biochem. Sci.* **21,** 197–198 (1996).
12. Belmont, L. D. & Mitchison, T. J. Identification of a protein that interacts with tubulin dimers and increases the catastrophe rate of microtubules. *Cell* **84,** 623–631 (1996).
13. Marklund, U., Larsson, N., Gradin, H. M., Brattsand, G. & Gullberg, M. Oncoprotein 18 is a phosphorylation-responsive regulator of microtubule dynamics. *EMBO J.* **15,** 5290–5298 (1996).
14. Heald, R. *et al.* Self-organization of microtubules into bipolar spindles around artificial chromosomes in *Xenopus* egg extracts. *Nature* **382,** 420–425 (1996).
15. Maucuer, A., Moreau, J., Mechali, M. & Sobel, A. Stathmin gene family: phylogenetic conservation and developmental regulation in *Xenopus*. *J. Biol. Chem.* **268,** 16420–16429 (1993).
16. Mayer-Jaekel, R. E. & Hemmings, B. A. Protein phosphatase 2A—a 'ménage à trois'. *Trends Cell Biol.* **4,** 287–291 (1994).
17. Tournebize, R. *et al.* Distinct roles of PP1 and PP2A-like phosphatases in control of microtubule dynamics during mitosis. *EMBO J.* (in the press).
18. Félix, M. A., Cohen, P. & Karsenti, E. Cdc2 H1 kinase is negatively regulated by a type 2A phosphatase in the *Xenopus* early embryonic cell cycle: evidence from the effects of okadaic acid. *EMBO J.* **9,** 675–683 (1990).
19. Larsson, N., Melander, H., Marklund, U., Osterman, O. & Gullberg, M. G2/M transition requires multisite phosphorylation of oncoprotein 18 by two distinct protein kinase systems. *J. Biol. Chem.* **270,** 14175–14183 (1995).
20. Sawin, K. E. & Mitchison, T. J. Poleward microtubule flux in mitotic spindles assembled *in vitro*. *J. Cell Biol.* **112,** 941–954 (1991).
21. Walczak, C. E., Mitchison, T. J. & Desai, A. XKCM1: a *Xenopus* kinesin-related protein that regulates microtubule dynamics during mitotic spindle assembly. *Cell* **84,** 37–47 (1996).
22. Samanta, A. & Greene, M. I. A kinase associated with chromatin that can be activated by ligand-p185$^{c\text{-}Neu}$ or epidermal growth factor-receptor interactions. *Proc. Natl Acad. Sci. USA* **92,** 6582–6586 (1995).
23. Ookata, K. *et al.* Cyclin B interaction with microtubule-associated protein 4 (MAP4) targets p34CdC2 kinase to microtubules and is a potential regulator of M-phase microtubule dynamics. *J. Cell Biol.* **128,** 849–862 (1995).
24. Masson, D. & Kreis, T. E. Binding of E-MAP-115 to microtubules is regulated by cell cycle-dependent phosphorylation. *J. Cell Biol.* **131,** 1015–1024 (1995).
25. Andersen, S. S. L., Buendia, B., Domínguez, J. E., Sawyer, A. & Karsenti, E. Effect on microtubule dynamics of XMAP230, a microtubule-associated protein present in *Xenopus laevis* eggs and dividing cells. *J. Cell Biol.* **127,** 1289–1299 (1994).
26. Vernos, I. *et al.* Xklp1, a chromosomal *Xenopus* kinesin-like protein essential for spindle organization and chromosome positioning. *Cell* **81,** 117–127 (1995).
27. Lombillo, V. A., Nislow, C., Yen, T. J., Gelfand, V. I. & McIntosh, J. R. Antibodies to the kinesin motor domain and CENP-E inhibit microtubule depolymerizaiton-dependent motion of chromosomes *in vitro*. *J. Cell Biol.* **128,** 107–115 (1995).
28. Félix, M. A., Clarke, P., Coleman, J., Verde, F. & Karsenti, E. in *The Cell Cycle: a Practical Approach* (eds Fantes, P. & Brooks, R.) 253–283 (IRL, New York, 1994).
29. Shamu, C. E. & Murray, A. W. Sister chromatin separation in frog egg extracts requires DNA topoisomerase II activity during anaphase. *J. Cell Biol.* **117,** 921–934 (1992).
30. Curmi, P. A. *et al.* The Stathmin tubulin interaction *in vitro*. *J. Biol. Chem.* (in the press).

Acknowledgements. We thank D. Chrétien, K. Dejgaard, J. Domínguez, R. Heald, J. Howard, T. J. Mitchison, I. T. Möst, A. Nebreda, M. Way, T. Wittmann and M. Zerial for discussions and reagents.

Correspondence and requests for materials should be addressed to S.S.L.A. (e-mail: andersen@embl-heidelberg.de).